Title	An Investigation into Scalpel Blade Sharpness Using Cutting Experiments and Finite Element Analysis
Authors(s)	McCarthy, Conor T., Hussey, M., Gilchrist, M. D.
Publication date	2005-09-15
Publication information	McCarthy, Conor T., M. Hussey, and M. D. Gilchrist. "An Investigation into Scalpel Blade Sharpness Using Cutting Experiments and Finite Element Analysis." Trans Tech Publications, September 15, 2005. https://doi.org/10.4028/www.scientific.net/KEM.293-294.769.
Publisher	Trans Tech Publications
Item record/more information	http://hdl.handle.net/10197/5929
Publisher's version (DOI)	10.4028/www.scientific.net/KEM.293-294.769
Notes	Additional RMSIDs: 5171035

Journal Citation (to be inserted by the publisher)

An Investigation into Scalpel Blade Sharpness using Cutting Experiments and Finite Element Analysis

C.T. McCarthy[1], M. Hussey[2], M.D. Gilchrist[3,*]

Dept. of Mechanical Engineering, University College Dublin, Ireland.

[1]conor.t.mccarthy@ucd.ie, [2]martin.hussey@ucd.ie, [3]michael.gilchrist@ucd.ie

*Corresponding Author

Keywords: Finite Element Analysis, Cutting, Indentation, Scalpel Blades, Sharpness.

Abstract: This paper presents an investigation into the sharpness of a surgical scalpel blade. An experiment was carried out in which a surgical scalpel blade was pushed through an elastomeric substrate at a constant velocity. The force-displacement characteristics were examined by plotting the stiffness as a function of blade displacement and it was found that this curve could clearly identify the point where the material separates to form a cut. A blade sharpness measurement was defined as the energy required to initiate an opening or cut in the substrate. A finite element model was developed to examine the stress state in the substrate at the point where the opening initiates. The development of this model is described. The model was validated against the experiment and close agreement was obtained. The von-Mises stress distribution under the blade tip was plotted and it was shown that the peak stress actually occurs away from the blade tip, suggesting that material separation would initiate away from the substrate surface.

Introduction

The *sharpness* of a cutting instrument is an important parameter to consider in all cutting applications because it strongly influences the mechanics of cutting, life of the cutting edge and surface finish or quality of the cut surface. A number of studies in diverse areas such as surgery [1,2], meat processing [3,4] and manufacturing [5,6] have used the term *sharpness* to describe the performance of a cutting instrument. However, in these papers the definition of sharpness has differed significantly. For example, in [1-3] sharpness was identified by the amount of force (i.e. maximum, initial etc.) exerted by the cutting instrument (blade) during a cutting trial, while in [5,6] it was defined by the radius of the cutting edge.

There is, as yet, no standard definition, measurement or protocol to quantify the sharpness of a cutting instrument, due to the complexity and diversity of the variables associated with cutting edge profiles [7]. This issue is being investigated by the authors [8] who are examining the cutting of bio-materials with surgical instruments such as scalpel blades and osteotomes. There are two aspects to this, the first being an investigation into factors affecting the cutting process using experimental and finite element techniques, with the aim of deriving a sharpness metric. The second, collaborative strand [9,10], involves developing a novel non-contact device to measure the sharpness of straight edge blades. This present paper is concerned with the first aspect of this project, i.e. an investigation of the cutting process and the derivation of a sharpness metric. An experiment and finite element model used to examine the cutting process are described.

Problem Description

The objective of this study is to establish a suitable parameter for quantifying the sharpness of a surgical blade. The approach taken is to force a surgical blade through an elastomeric substrate and observe the forces generated. A polyurethane rubber with a Shore hardness of 40 was chosen as the substrate material and will subsequently be referred to as the substrate material. The blade chosen for the study is a Swann-Morton No. 16 surgical scalpel blade. The Finite Element (FE) model is constructed in the non-linear FE code ABAQUS [11].

After, the experimental results are presented a suitable measure of blade sharpness is defined. Next, the development of the finite element model, including the characterisation of a non-linear material model is described. The FE model is then validated against the experiments. Finally, the FE model is used to examine the stress state in the elastomer at the point where the cut initiates.

Experimental Cutting Tests

An experiment was carried out to examine the forces generated when cutting the substrate with a scalpel blade. A test rig was designed, manufactured and fitted into a Tinius-Olsen universal testing machine, and is shown in Fig. 1. The lower part held the substrate material tightly between two anti-buckle guides while the upper part held the scalpel blade and handle and was attached to the moving cross-head of the testing machine. The blade was pushed through the substrate material at a quasi-static rate of 5 mm/min and the reaction force was measured by the load cell mounted above the blade clamp. The blade displacement was measured using an extensometer.

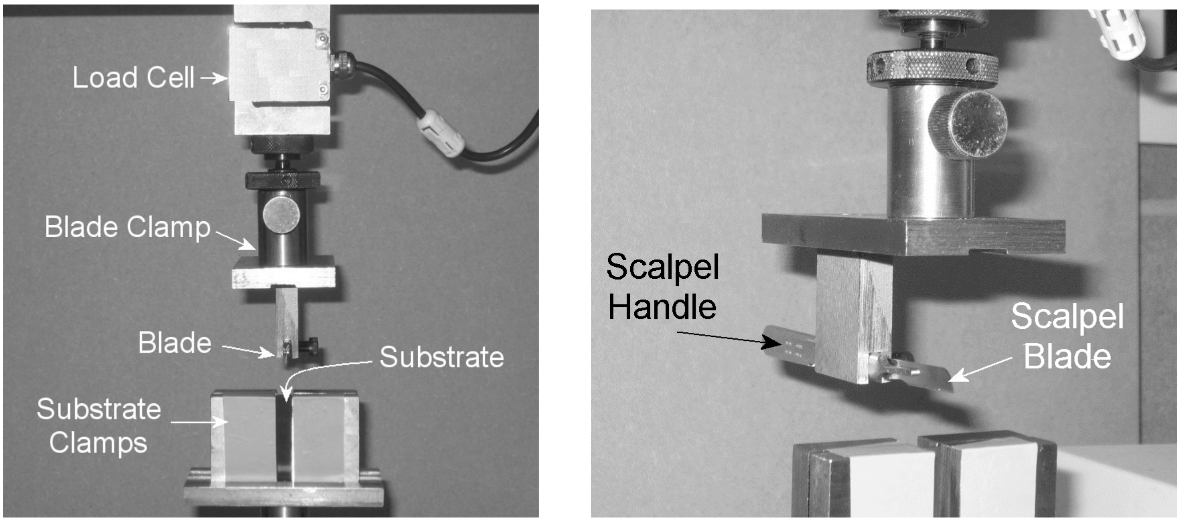

Figure 1: Experimental set-up for the cutting trials

For repeatability, three tests were performed with a new blade being used for each test. The resulting load-deflection curves are shown in Fig. 2(a). As can be seen, the curves rise in a non-linear manner to approximately 2 mm blade displacement. The three tests are in good agreement up to this point. The curves then deviate but remain linear until about 12 mm blade displacement. Again, good agreement between the tests is obtained with small differences in stiffness observed. After 12 mm blade displacement the curves become non-linear and oscillate around the 30 N load level.

To examine the characteristics of the cutting process the slope of each test in Fig. 2(a) is plotted as a function of blade displacement in Fig. 2(b). These curves highlight some interesting features of the cutting process. Firstly, the stiffness rises linearly up to 2 mm blade displacement, at which point the curves become essentially constant. From a separate test in which the blade was progressively lowered in 0.1 mm increments and then retracted to allow the substrate to be examined, it was found that the point where the stiffness curve becomes constant (i.e., point A in Fig. 2(b)) corresponds to the point were a cut initiates in the substrate. The curves remain constant until approximately 7.5 mm blade displacement and then start to reduce. This point represents the onset of steady state cutting. At approximately 16 mm blade displacement, the stiffness curves reduce to zero and this represents the point when fully established steady state cutting is reached, i.e., where the cutting forces become constant (around a mean value of approximately 30 N, as shown in Fig. 2(a)).

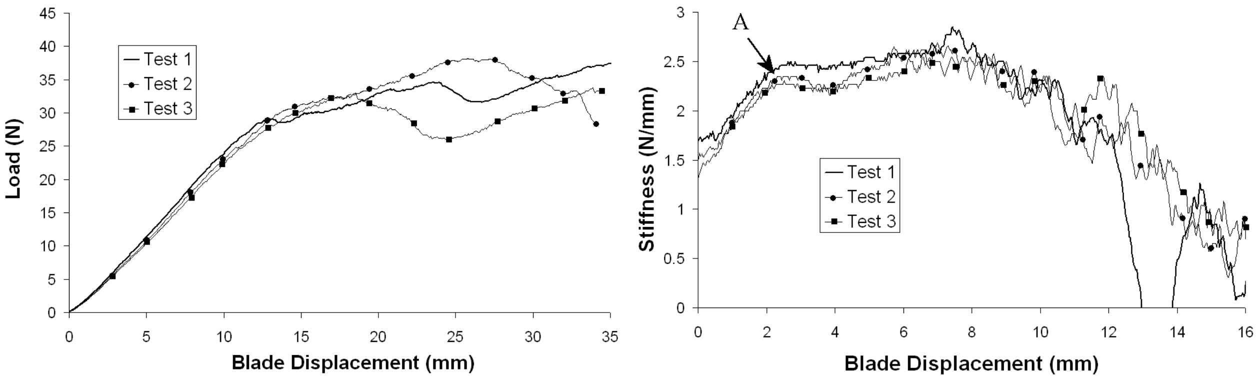

(a) Load-Deflection Curves **(b) Stiffness Curves**

Figure 2 Results from the experimental cutting trials

Blade Sharpness Measurement

It is postulated that the energy required to initiate a cut in the substrate could be used as a measure of blade sharpness. To examine this, the cutting energy, E, was determined from Fig. 2(a) by integrating the load deflection curve using the following equation:

$$E = \int_{x_0}^{\delta} F dx \approx \frac{1}{2} \sum_{i=1}^{N} (x_{i+1} - x_{i-1}) F_i \qquad (1)$$

where: F_i and x_i are the force and displacement at experimental data point i, x_o is the displacement where the force just starts to rise, δ is the blade displacement at which the cut initiates and was determined from Fig. 2(b) as 2 mm and N is the total number of data points up to 2 mm displacement. Table 1 shows the results for the cut initiation energies from the tests. As can be seen good agreement between each test was obtained, which was due to using a new blade for each test.

Table 1 Cut initiation energy for each test

Test	Cut Initiation Energy (N-mm)	Average	Standard Deviation
1	3.87		
2	3.58	3.62	0.232 (6.4%)
3	3.41		

Finite Element Model

The FE model of the experiment is shown in Fig. 3(a). Due to symmetry, only half the blade and substrate were modelled. To capture the near singular stress state under the blade tip a very fine mesh (not shown) was used to discretise the substrate. A state of plane stress was assumed and hence fully integrated plane stress elements (CPS4) were used for the substrate. To simulate the support plate and anti-buckle guides, two sides of the plate were fixed (i.e. $u = v = 0$) as shown. A symmetry boundary condition was used to enforce symmetry along the left edge of the model. As with the experiment the remaining edge was free to displace. The geometry of the blade was determined from micrographs as shown in Fig. 3(b) and was modelled using a rigid contact body, as shown in Fig. 3(c). To avoid applying point loads, the blade tip was rounded with a radius of 10 μm. The motion of the blade was specified via a contact control node.

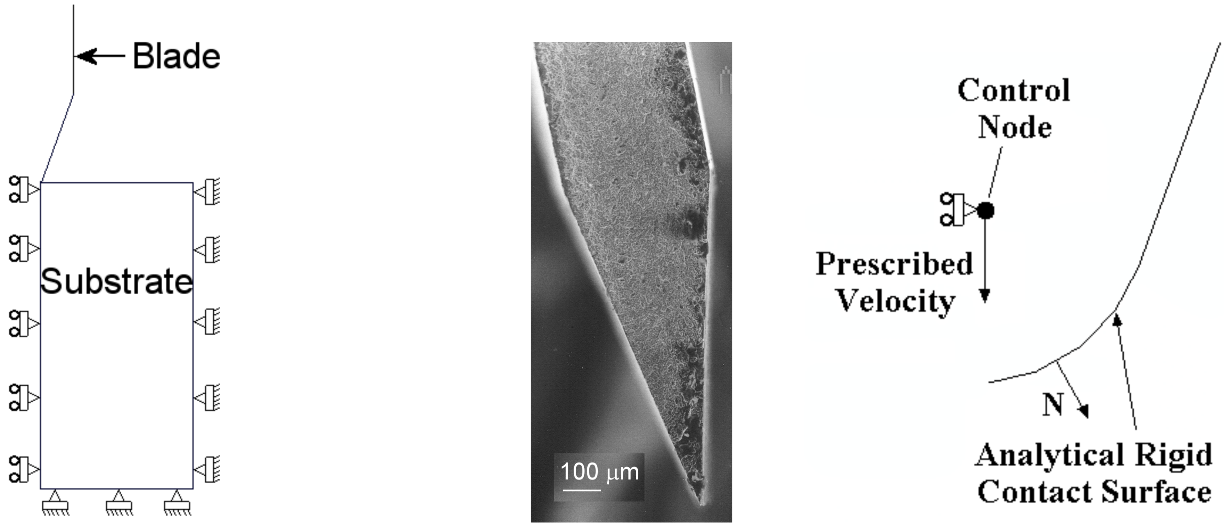

(a) (b) (c)

Figure 3: Finite element model development, (a) Geometry and boundary conditions, (b) Micrograph of the blade, (c) boundary conditions on rigid contact body (blade)

Material Model

To model the non-linear behaviour of the elastomeric substrate an Ogden [12] strain energy density function was employed. The material used in this study was assumed to be incompressible and the corresponding form of the Ogden strain energy density function, W, is:

$$W = \sum_{i=1}^{N} \frac{2\mu_i}{\alpha_i^2}\left[\lambda_1^{\alpha_i} + \lambda_2^{\alpha_i} + \lambda_3^{\alpha_i} - 3\right] \tag{2}$$

where μ_i and α_i are material constants, λ_j (j =1,2,3) are the principal stretch ratios and N is the function order. The incompressibility assumption means that volume is conserved, thus:

$$\lambda_1\lambda_2\lambda_3 = 1 \tag{3}$$

Hence there are only two independent variables remaining. For a uni-axial stretch in the 1-direction:

$$\lambda_1 = \lambda \text{ and } \lambda_2 = \lambda_3 \tag{4}$$

By substitution of Eq. 3 and Eq. 4 into Eq. 2, a constitutive equation for a uni-axial deformation can be determined as:

$$\sigma_{true} = \lambda\frac{\partial W}{\partial \lambda} = \sum_{i=1}^{N} \frac{2\mu_i\lambda}{\alpha_i}\left[\lambda^{(\alpha_i - 1)} - \frac{1}{\lambda^{\left(1+\frac{\alpha_i}{2}\right)}}\right] \tag{5}$$

where σ_{true} is the true or Cauchy stress. Uni-axial tensile tests were performed on the substrate and a result is shown in Fig. 4. Non-linear regression was used to fit Eq. 5 to the experimental result and a good fit was obtained with $N = 3$, $\alpha_1 = 2.28$, $\alpha_2 = 22.5$, $\alpha_3 = -1.98$, $\mu_1 = 0.27$, $\mu_2 = 1e - 16$, and $\mu_2 = 0.4$. To test the suitability of the derived material constants, a single element plane stress FE model was constructed. Boundary conditions that enforced a uni-axial stretch were applied and the resulting Cauchy stress is plotted in Fig. 4. As can be seen close agreement with the experiment was obtained, thus providing confidence that the material model, finite element type and solver were behaving accurately. The one element model was also used to examine the compressive (0 $< \lambda < 1$, shown in Fig. 4) and equi-biaxial ($\lambda_1 = \lambda_2 > 1$, not shown) deformation modes. Currently, tests are being performed to verify the material model in these deformation modes.

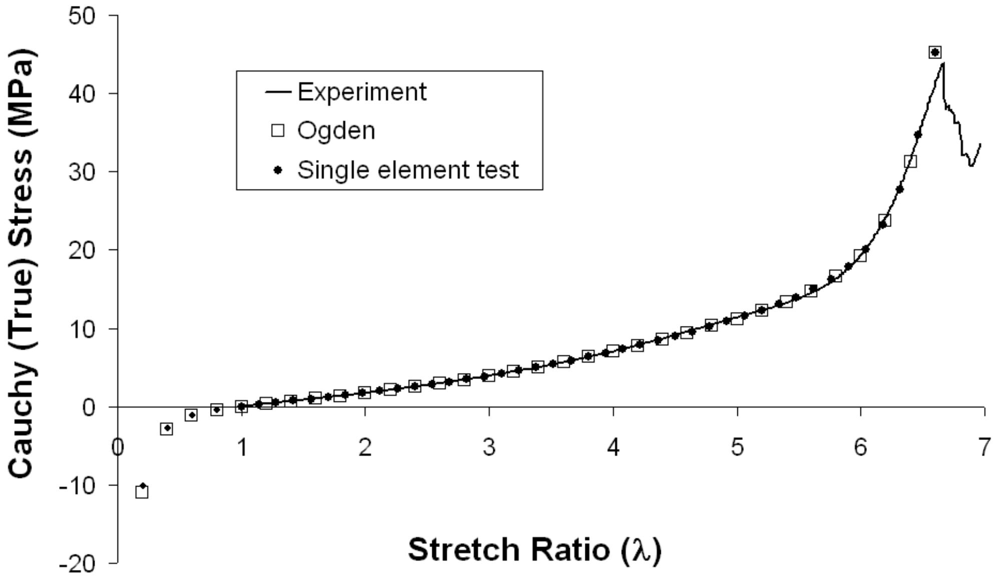

Figure 4: Uni-axial deformation of the elastomeric substrate. Figure also shows the Ogden model (Eq. 5) and single element FE test

Surface Interaction Model

An important aspect of the model was to correctly account for surface interaction between the blade and substrate. As large displacements were expected in the substrate, a finite sliding contact algorithm which allows for arbitrary separation, sliding and rotation between surfaces was used.

Friction between the blade and substrate was introduced using the following exponential law:

$$\mu = \mu_k + (\mu_s - \mu_k)e^{-d\dot{\gamma}} \tag{6}$$

where μ_k and μ_s are the kinetic and static coefficients of friction respectively, d is a user defined decay coefficient and $\dot{\gamma}$ is the slip rate between the two surfaces. It is outside the scope of this work to measure the coefficient of friction between the blade and substrate and so it was estimated as $\mu_s = 0.3$, $\mu_k = 0.25$ and $d = 0.9$.

Model Validation

To validate the proposed model, the deformed shape and load-deflection response are compared to the experiment. The blade displacement level chosen for comparison is 2 mm, i.e. at the point where the "cut" just initiates. A full field view of the deformed shape is shown in Fig. 5. A can be seen the deformation characteristics in the model are very similar to the experiment. To provide a more quantitative comparison, the vertical displacement of the top edge for the experiment and model was plotted as shown in Fig. 6. Good agreement between the model and experiment is seen. Fig. 7 shows the load-displacement plots from the model and experiment. Again, good agreement is obtained. However, the experiment is less stiff than the model, which was due to some slipping of the substrate in the grips (the model assumed a perfectly clamped boundary, see Fig. 3). In summary, the proposed model was considered to have been validated and sufficiently accurate to proceed with examining the stress state at the on-set of cut formation.

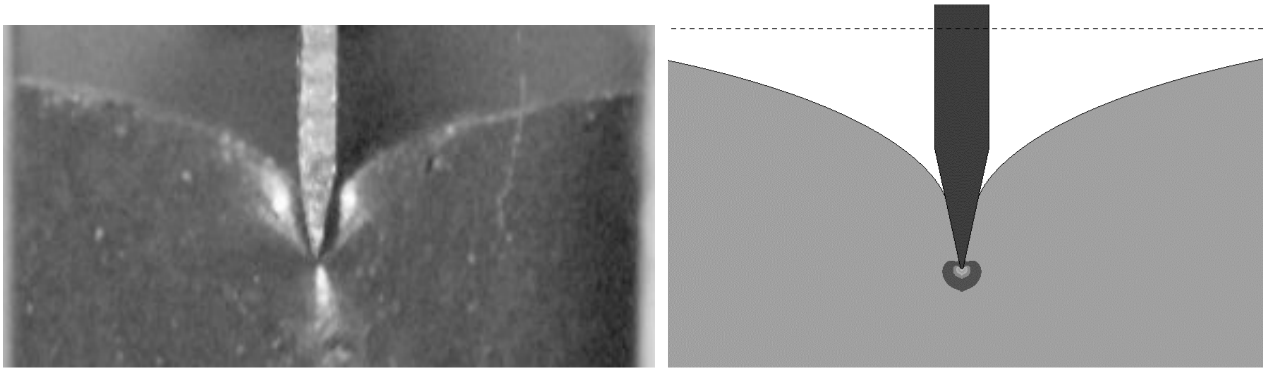

(a) Experiment (b) Simulation

Figure 5 Deformed shape at a blade displacement of 2 mm (pictures not to same scale)

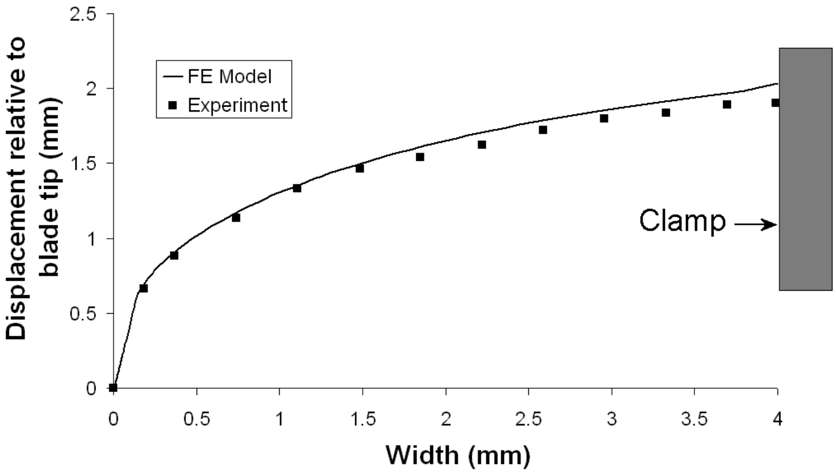

Figure 6 Vertical displacement of the free edge (i.e., top) in the experiment and model

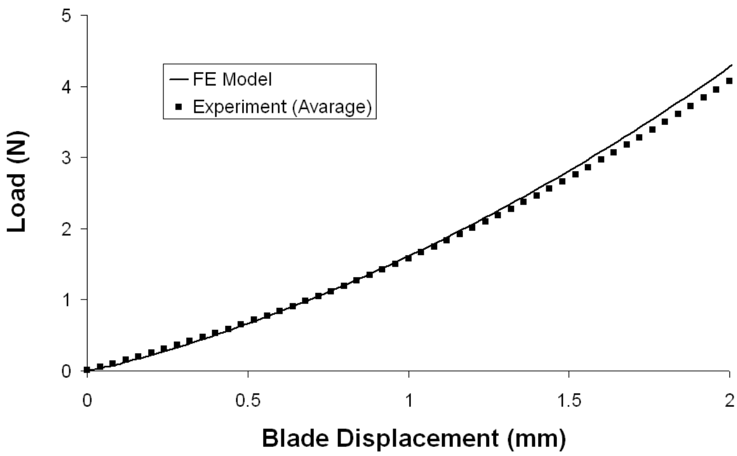

Figure 7 Load – displacement response for the experiment and model

FE Results

Firstly, the blade sharpness from the model was determined from Fig. 7 using Eq. 1 as 3.73 N-mm. This is only a 3% overestimation of the average experimental value of 3.62 N-mm (see table 1).

A drawback with determining a sharpness measurement from the model is that the cut initiation displacement (i.e. δ in Eq. 1) has to be determined experimentally. To avoid this pitfall, the validated model is used to examine the stress state in the substrate at the onset of the cut formation (i.e. a blade indentation of 2 mm) so as to determine a failure stress level. The path for plotting the stress is shown graphically in Fig. 8(a). Fig. 8(b) shows the von-Mises stress distribution in the substrate under the blade tip (along the path shown in Fig. 7). It should be noted that the blade tip radius is 10 μm. As can be seen, the von-Mises stress directly under the blade tip (i.e. $x = 0$) is approximately 12 MPa, which is considerably lower than the failure stress for this material (the failure stress was determined from Fig. 4 as approximately 44 MPa.). However, the stress rises sharply directly below the substrate surface, reaching a peak of approximately 34 MPa (which is closer to the failure stress in uni-axial tension) only 0.01 mm away from the blade tip, before falling off again. This stress state suggests that failure would initiate below the substrate surface. This peak failure stress of 34 MPa will be used to evaluate the sharpness of other blade profiles using the developed model and this will be reported on in a later publication.

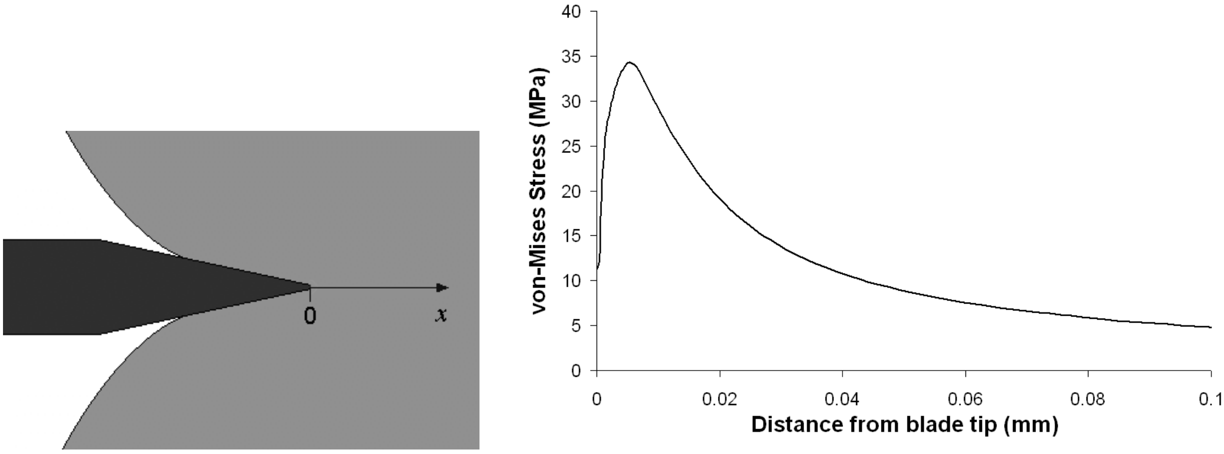

(a) Path for Plotting Stresses **(b) von-Mises Stress Distribution**

Figure 8 von-Mises Stress distribution under the blade tip at 2 mm blade indentation

Conclusion

An experiment was carried out in which a surgical scalpel blade was pushed through an elastomer at a constant velocity. The force-displacement characteristics were examined by plotting the stiffness as a function of blade displacement and it was found that this curve could identify the point where a cut initiates in the substrate. A measure of blade sharpness was defined as the energy required to initiate this cut. This sharpness measure may be useful to other researchers for examining the quality of blades or wear on blades.

A finite element model was constructed to examine the stress state in the substrate at the point where the cut initiates. By comparing deformed shape and load-deflection characteristics, the model was successfully validated against the experiment. The von-Mises stress distribution directly under the blade tip was examined and it was shown that the peak stress in the substrate actually occurs ahead of the blade tip. This suggests that the cut would initiate within the substrate and not at the surface. It was found that the peak von-Mises stress at cut formation was 34 MPa (which is less that the uni-axial strength of the material) and this value will be used to compare and assess the sharpness of other blade profiles.

Acknowledgments

The authors acknowledge Enterprise Ireland for funding this research under the auspices of the Commercialisation Fund (ATRP/2002/422B).

References

1. Watkins, F.H., London, S.D., Neal, J.G., Thacker, J.G., Edlich, R.F., Biomechanical performance of cutting edge surgical needles. J. Emergency Medicine 1997; 15(5):679-685.
2. Thacker, J. G., Rodeheaver, G. T., Towler, M. A., Edlich, R. F., Surgical needle sharpness. The American Journal of Surgery 1989; 15(9):334-339
3. McGorry, R.W., Dowd, P.C., Dempsey, P.G., Cutting moments and grip forces in meat cutting operations and the effect of knife sharpness. Applied Ergonomics 2003; 34:375-382.
4. King, M.J., Knife and impact cutting of lamb bone. Meat Science 1999; 52:29-38.
5. Yuan, J. J., Zhou, M., Dong, S., Effect of diamond tool sharpness on minimum cutting thickness and cutting surface integrity in ultraprecision machining. J. of Mat. Proc. Tech. 1996; 62(4):327-330.
6. Abdel Moneim, M. Es., Tool edge roundness in finish machining at high cutting speeds. Wear 1980; 58(1):173-192.
7. Reilly, G.A., McCormack, B.A.O., Taylor, D., Cutting sharpness measurement: a critical review. J. Mat. Proc. Tech. 2004. *In Press.*
8. McCarthy, C.T., E. O'Dwyer, N.P. O'Dowd, M. Hussey, M.D. Gilchrist, A Numerical and Experimental Investigation into the Forces Generated when Cutting Biomaterials. ASM-International Conference on Materials & Processes for Medical Devices. Minnesota, USA. 25-27 August, 2004. In-Press.
9. Price, E., Reilly, G.A., McCormack, B.A.O., Macey, A., Techniques for investigation of surgical cutting instruments. Proc. ASM Materials & Processes for Medical Devices Conf., Minnesota, August 25-27, 2004.
10. Doran, C., McCormack, B.A.O., Macey, A., A model of the failure process of skin during cutting. Proc. ASM Materials & Processes for Medical Devices Conf., Minnesota, August 25-27, 2004.
11. Hibbitt, Karlsson & Sorensen Inc., 2004, ABAQUS version 6.4-1.
12. Ogden, R.W. Large Deformation Isotropic Elasticity: On the Correlation of Theory and Experiment for Incompressible Rubberlike Solids, Proc. Royal Society, Vol. A (326), pp. 565-584, 1972.
13. Anderson, J., Birkbeck, A., Tomson, R., Computational modelling of penetration of biomaterials by a sharp knife. Modern Practise in Stress and Vibrations Analysis, Gilchrist, M.D.,(ed.). Proc. 3rd International Conference on Modern Practice in Stress and Vibration analysis, University College Dublin, Ireland 1997. pp 347-353.
14. Shih, A.J., Finite Element analysis of the rake angle effects in orthogonal metal cutting, Int. J. Mech. Sci. 1996; 38(10):1-17.